THE JOURNAL OF PHYSICAL CHEMISTRY C

Article

pubs.acs.org/JPCC

Formation of $RuO(OH)_2$ on RuO_2-Based Electrodes for Hydrogen Production

Lars-Åke Näslund,*[,†] Árni S. Ingason,[†] Susanne Holmin,[‡,§] and Johanna Rosen[†]

[†]Materials Design, Thin Film Physics Division, Department of Physics, Chemistry, and Biology (IFM), Linköping University, SE-581 83 Linköping, Sweden

[‡]Permascand AB, SE-840 10 Ljungaverk, Sweden

[§]Department of Natural Sciences, Mid-Sweden University, SE-870 10 Sundsvall, Sweden

ABSTRACT: The catalytic and durable electrode coating of ruthenium dioxide (RuO_2), applied on nickel (Ni) substrates, is today utilized as electrocatalytic cathodes for hydrogen production, e.g., in the chlor-alkali process and alkaline water electrolysis. The drawback is, however, the sensitivity to reverse currents obtained during power shutdowns, e.g., at maintenance, where the RuO_2-based electrodes can be severely damaged unless polarization rectifiers are employed. Through the material characterization techniques X-ray diffraction and X-ray photoelectron spectroscopy, we can now reveal that RuO_2 coatings, when exposed to hydrogen evolution at industrially relevant conditions, transforms into ruthenium oxyhydroxide ($RuO(OH)_2$). The study further shows that as the hydrogen evolution proceeds the formed $RuO(OH)_2$ reduces to metallic ruthenium (Ru).

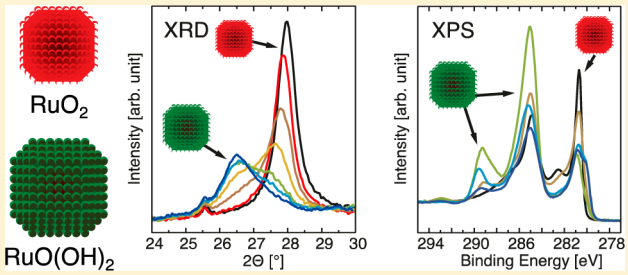

1. INTRODUCTION

The catalytic and durable electrode coatings of ruthenium dioxide (RuO_2) or mixtures of RuO_2 and other metal oxides, e.g., titanium dioxide (TiO_2) and iridium dioxide (IrO_2), are widely employed in a large variety of industrial electrochemical processes, such as chlor-alkali and chlorate processes, water treatment, electrowinning, and water electrolysis.[1,2] As a functionalized anode, RuO_2-based electrodes are often referred to as dimensionally stable anodes (DSA) and has been utilized for more than four decades. In addition, these types of electrodes have also found practical applications as electrocatalytic cathode for hydrogen production, e.g., in the chlor-alkali process and alkaline water electrolysis,[3,4] where the latter represents a promising candidate for a convenient route for energy storage and conversion.[5]

However, as a RuO_2-based cathode for hydrogen production there is a stability issue manifested as a coating loss when the cathode is exposed to reverse currents at power shutdowns, e.g., for maintenance. Several studies have, in addition, reported loss of coating material when performing polarity inversion tests, i.e., repetitive cycling of the current or potential between the hydrogen and oxygen evolution reaction or by applying an anodic current after extensive hydrogen evolution.[6−9] The reason for the loss of coating material has, to our knowledge, not previously been investigated, although it has been suggested that during hydrogen evolution in alkaline media RuO_2 reduces through hydration or hydroxylation processes.[8,10−12]

The aim of the present work is to reveal the chemical process behind the destabilization of the RuO_2 coating when extensively exposed to hydrogen evolution. The material characterization techniques employed in the study are X-ray diffraction (XRD) for crystal structure information on the electrode material and X-ray photoelectron spectroscopy (XPS) for chemical environment information around the probed element. While the bulk probing XRD provides phase-specific information on the array of atoms in the material, the surface probing XPS provides element-specific information on the electronic structure of the examined components.

An X-ray diffraction study of RuO_2/Ni electrodes for hydrogen production has previously been performed by Iwakura et al.,[8] which showed that the intensity of the RuO_2 (110) peak decreased with time when the cathode was exposed to hydrogen evolution at 3 kA/m^2 and 90 °C in 10 M NaOH electrolyte. In addition the peak in the RuO_2 (110) region was shifted toward lower angles, which the authors speculated being caused by a partial reduction of the RuO_2 to lower valence oxides such as RuOOH. While the former study followed the RuO_2 (110) peak progress for 18 h, Hachiya et al.[12] spent 180 days of hydrogen evolution at 6 kA/m^2 and 90 °C in 32 wt % NaOH electrolyte. In the end of the study, it was concluded that the RuO_2 peaks in the XRD diffractogram were replaced with peaks that were assigned to hydrated RuO_2. In addition there was a weak feature indicating the presence of metallic Ru. Earlier studies have, thus, shown that RuO_2 transforms into a new phase, although it has not yet been unambiguously identified.

To identify the phase transformation the RuO_2/Ni electrodes have previously been investigated through XPS,[10,13,14] and the

Received: April 23, 2014
Revised: June 19, 2014
Published: June 20, 2014

   dx.doi.org/10.1021/jp503960q | J. Phys. Chem. C 2014, 118, 15315−15323

studies suggest a hydroxylation process, mainly because of the observed intensity redistribution in the O 1s spectrum. As for many transition metal oxides, interpretation of the Ru 3d spectrum of RuO_2 is not a straightforward procedure. Figure 1

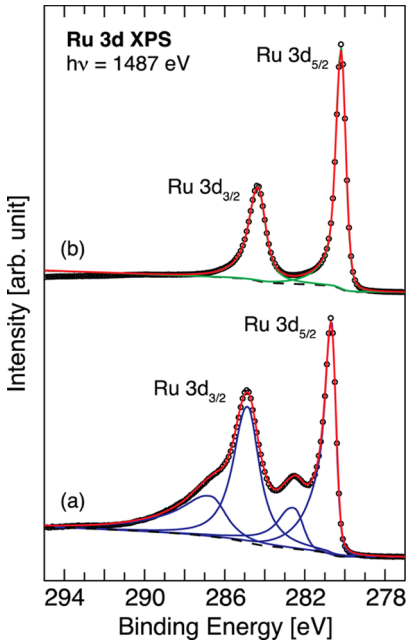

Figure 1. Ru 3d XPS of (a) the reference RuO_2/Ni coating and (b) Ru-metal, fitted with four and two asymmetric Gaussian−Lorentzian curves, respectively, on Shirley backgrounds. The peak fitting is performed according to section 2.4.

shows the Ru 3d XPS spectra for Ru-metal and for a RuO_2/Ni coating which are obtained according to section 2.3. The Ru 3d XPS spectrum for the Ru-metal shows $3d_{5/2}$ and $3d_{3/2}$ at 280.2 and 284.3 eV binding energies, respectively, while the RuO_2/Ni coating features the two primary spin−orbit components at 280.7 and 284.9 eV, respectively. Most noticeable is that the full with at half-maximum (fwhm) for the Ru $3d_{3/2}$ peak is about twice as large as the Ru $3d_{5/2}$ peak, which is attributed to a Coster−Kronig broadening.[15] The larger fwhm is, thus, ascribed to the Ru $3d_{3/2}$ photoelectron process that opens up an M4M5N45 Coster−Kronig decay channel; i.e., the electron core hole in the M shell is filled by an electron from a higher subshell of the same shell while releasing energy through an Auger electron from the N-shell. The inner shell decay channel will reduce the lifetime of the Ru $3d_{3/2}$ hole state leading to an increased core hole lifetime broadening of the Ru $3d_{3/2}$ peak, i.e., a $3d_{3/2}$ peak that has a larger fwhm compare to the $3d_{5/2}$ peak. Furthermore, the XPS spectrum for the RuO_2/Ni coating shows, in addition to the dominant low binding energy spin−orbit doublet, two satellites at 282.5 and 286.8 eV, respectively, which are attributed to final-state screening effects derived from the strong Coulomb interaction between valence electrons and the core hole produced in the photoionization process.[16,17] Metallic transition metal components can undergo a change in the core hole screening from mainly extended sp-band screening to mainly localized d-level screening that results in two different final states, very often denoted unscreened and well-screened, respectively.[18] The photoelectron can leave the atom before or after the change in the core hole screening and subsequently show main lines and satellites as complex features in the XPS spectrum, where the more efficient localized d-level screening gives rise to the low binding energy spin−orbit doublet that in this work is identified as main peaks.

With a confident assignment of all features in the Ru 3d XPS spectra of Ru-metal and RuO_2/Ni coating it has in the present work been possible to identify the chemical process involved when RuO_2 coatings, exposed to hydrogen evolution at industrially relevant conditions, degenerates and forms new chemical species sensitive to reverse current.

2. EXPERIMENTAL SECTION

2.1. RuO_2 Coating Preparation. Most RuO_2-based electrodes are produced through thermal decomposition of ruthenium chloride ($RuCl_3$) salt solutions on a conductive metal substrate electrode and for alkaline water electrolysis the most common substrate is nickel (Ni), mainly because of its high corrosion resistance to highly concentrated alkaline electrolyte at elevated temperatures. A precursor solution containing 0.60 M Ru was prepared from $RuCl_3 \cdot nH_2O$ salt from Heraeus (40.27 wt % Ru, analytical reagent grade) and 1-propanol from Fischer Scientific (analytical reagent grade). Ni disks (Ni-201) with a diameter of 25 mm and thickness of 1 mm were pretreated to achieve acceptable adhesion strength of the RuO_2 coating to the Ni substrate. The pretreatment included blasting with Al_2O_3 particles (diameter: 50−75 μm), ultrasonically cleaning in Milli-Q water for 10 min at 30 °C, and rinsing in acetone.

The RuO_2 coating was prepared by a conventional multistep precursor solution application/calcination method. A total of 100 μL of the precursor solution was applied on the Ni disks and left for 2.5 min. Spin coating was then performed at 4500 rpm for 30 s. Thereafter the sample was dried in air for 5 min at room temperature and 5 min at 80 °C followed by 12 min calcinations at 500 °C. This procedure was repeated four times to obtain superimposed layers of RuO_2 with a thickness of 0.4−1.4 μm at the thinnest and thickest regions, respectively. On the fourth application cycle the heat treatment at 500 °C was prolonged to 1 h. Using the described spin coating application technique, the obtained metal loading became 4.5 ± 0.2 g Ru/m^2.

2.2. Electrochemical Setup. The electrochemical cell consisted of three electrodes where the RuO_2-coated Ni disk (cut to a size of 3.1 cm^2), a Ni mesh, and a standard calomel electrode (sat. KCl) from Radiometer Copenhagen were used as a working electrode, a counter electrode, and a reference electrode, respectively. The RuO_2-coated Ni disks and the Ni mesh were attached to conductors in the form of 25 cm long Ni rods (diameter 1.5 mm) welded to the top end of the electrodes and mounted in the electrochemical cell at a distance of 4 cm from each other. The reference electrode, on the other hand, was operated through a Luggin capillary connected from an external assembly.

The electrochemical cell was prepared with a newly made RuO_2/Ni electrode, fresh 8 M NaOH electrolyte and heated to 90.0 ± 0.2 °C prior to each hydrogen evolution run. The electrolyte was prepared from NaOH pellets obtained from Scharlau (reagent analytical grade) dissolved in Milli-Q water. To minimize the effect of mass transport limitation on the electrode surface caused by strong gas evolution, the electrolyte was stirred continuously during each run. The hydrogen evolution was obtained through galvanostatic polarization at −6.4 kA/m^2.

2.3. Material Characterization. XRD for phase analysis was performed with an X'pert XRD system from Panalytical

dx.doi.org/10.1021/jp503960q | J. Phys. Chem. C 2014, 118, 15315−15323

using Ni-filtered Cu Kα radiation. Symmetric θ-2θ scans were operated using normal Bragg−Brentano geometry. Calibration of the 2θ scale was obtained through the Al_2O_3 (012)-peak, located at 25.577°. The observed Al_2O_3 peak is assigned to 50−75 μm particles incorporated into the surface of the Ni substrates prior to application of the precursor solution.

Chemical bonding states were probed through Ru 3d and O 1s XPS, which were performed with the AXIS Ultra^{DLD} system from Kratos using monochromatic Al Kα radiation. The binding energy scale of all XPS spectra presented here was calibrated against the Fermi-edge (E_f), which was set to a binding energy of 0 eV. The overall energy resolution obtained was better than 0.5 eV. Normalization of all spectra was performed at the background on the low binding energy side of the main peak/peaks.

2.4. XPS Spectrum Peak Fitting. XPS spectrum peak fitting of the Ru 3d XPS spectra for Ru-metal and for a RuO_2/Ni coating are performed using asymmetric Gaussian−Lorentzian (asym-GL) curves. The peak fitting procedure is constrained using an approach where the two main peaks, Ru $3d_{5/2}$ and Ru $3d_{3/2}$, have the same Gaussian but different Lorentzian contributions caused by the increased core hole lifetime broadening of the Ru $3d_{3/2}$ peak.[15] For the RuO_2/Ni coating the satellite features are fitted with asym-GL curves where the Lorentzian contribution is the same as obtained for the main peaks Ru $3d_{5/2}$ and Ru $3d_{3/2}$, respectively, but with twice as large Gaussian contribution compared to the main peaks. In addition, the two satellite features need to have the same binding energy shift relative to their main peak. Within these constraints the asym-GL curves were free to adjust position, height, Gaussian and Lorentzian contributions, and asymmetry.

Results from XPS spectrum peak fitting of the Ru-metal and the RuO_2/Ni coating are included in Figure 1, which shows that it is enough to use two and four asym-GL curves, respectively, for a reasonable good fit to the two Ru 3d XPS spectra. Since the samples have been exposed to air it is plausible that carbon contamination is present on the surfaces[19] and therefore show contributions of C 1s components, i.e., carbon (graphite) at 284.5 eV, hydrocarbon (−CH_2− and −CH_3) at 285.7 eV, and carboxylate (−COO) at 289.2 eV.[20] However, GL curves representing possible C 1s components were suppressed down to zero intensity when they were included. This might indicate that the carbon contamination on the Ru-metal and the RuO_2/Ni coating sample is at a very low level, or it might suggest that the C 1s features from carbon contamination are shifted toward higher binding energy compare to what expected and therefore is hidden under the Ru $3d_{3/2}$ component in the spectra. That C 1s contribution might be hidden under the Ru $3d_{3/2}$ of the RuO_2 spectrum may explain why the intensity distribution over the Ru 3d region shows a 3d doublet peak ratio of 3:3.8 instead of 3:2. On the other hand, the 3d doublet peak ratio of the Ru-metal is 3:2.1, which supports the suggestion of negligible amount of C 1s contamination on the samples. Alternative explanations for the extra high intensity in the Ru $3d_{3/2}$ region of the RuO_2/Ni coating could then be that the Shirley loss function, which is used for the background subtraction, does not represent the intrinsic loss structure well enough to completely remove the background contribution before the peak fitting,[21] the Ru $3d_{3/2}$ region of the RuO_2/Ni coating also consists of intensity from Ru $3d_{5/2}$ features, e.g., because of final-state screening effects,[18] or the electrode coating consists of hydrated or hydroxylated (or oxyhydroxylated) Ru-species with the Ru $3d_{5/2}$ component shifted into the Ru $3d_{3/2}$ region of RuO_2. The present study suggests the last.

The peak fitting of an XPS spectrum of a RuO_2/Ni electrode that has been exposed to hydrogen evolution was performed with a fitting procedure that included the experimentally obtained spectra of the reference RuO_2/Ni coating and the Ru-metal shown in Figure 1, four spectra of the RuO_2 main peaks obtained from the peak fitting of the reference RuO_2/Ni coating, an experimentally obtained spectrum of C 1s contamination on TiO_2, and a Shirley background for the peak fitted background-free RuO_2 main peaks. The experimentally obtained spectra of the reference RuO_2/Ni coating, the Ru-metal, and the C 1s contamination on TiO_2 were only free to adjust their intensity, while the RuO_2 main peaks (Ru $3d_{5/2}$ and Ru $3d_{3/2}$) obtained from the peak fitting of the reference RuO_2/Ni coating were free to adjust both their intensity and position on the binding energy (BE) scale (the intensity ratio and the BE difference between the Ru $3d_{5/2}$ and Ru $3d_{3/2}$ peaks were the same as obtained in the peak fitting of the reference RuO_2/Ni coating). No peaks were allowed to change their fwhm. This peak fitting procedure reduced the number of parameters significantly without losing meaningful information about the chemical environment around the probed Ru atoms and at the same time retaining the constrains used in the peak fitting of the RuO_2 reference, i.e., with the same Gaussian and Lorentzian contributions, peak asymmetries, and the relative BE positions and heights of the Ru $3d_{5/2}$ and Ru $3d_{3/2}$ spin−orbit components intact.

The peak fitting of the O 1s spectra assumed that six asym-GL curves must be included in the peak fitting procedure: one asym-GL curve that represents RuO_2, one asym-GL curve that represents H_2O, two asym-GL curves that represent the Ni−O components,[22] and two asym-GL curves that represent the unknown phase. In addition, the peak fitting were constrained in the way that each asym-GL curve, with the same shape and location, must be present in all fitted O 1s spectra.

Since the spectra originate from samples with a complex mixture of components, e.g., different chemical components, different core hole lifetime broadening for the different chemical components as well as for the $3d_{3/2}$ and the $3d_{5/2}$ spin−orbit components, different final state screening of the produced core hole, etc., the fit to the spectrum would be better with more peaks and with variations in peak shapes. However, the drawback would be that the important information for this study would be harder to extract from the crowd of peaks that would fill the figures. We have therefore selected to use the minimum number of peaks and peak shapes to highlight the important information gained from the peak fitting.

3. RESULTS AND DISCUSSION

3.1. X-ray Diffraction. Six newly made RuO_2/Ni electrodes were, with a current density of −6.4 kA/m^2, exposed to hydrogen evolution in a fresh 8 M NaOH electrolyte at 90.0 °C. The durations for hydrogen production for each RuO_2/Ni electrode were 0.5, 3, 6, 12, 18, and 24 h. The XRD diffractograms of the RuO_2 (110) peak region, presented in Figure 2, show that while exposed to hydrogen evolution the electrode coating transforms from the rutile phase RuO_2 into another phase. This phase transformation has previously not been identified, to our knowledge, although it has been observed in earlier studies.[8,12]

dx.doi.org/10.1021/jp503960q | J. Phys. Chem. C 2014, 118, 15315−15323

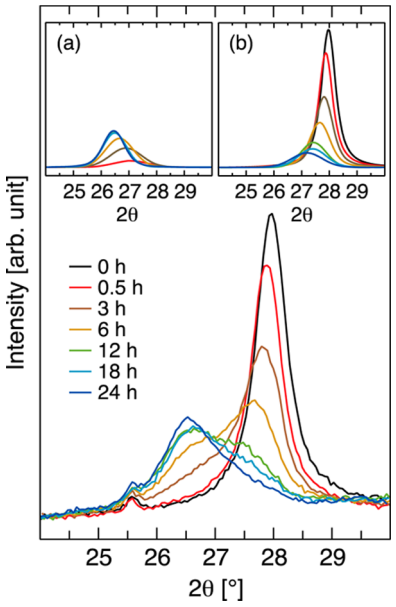

Figure 2. X-ray diffractograms of RuO_2/Ni electrodes exposed to hydrogen evolution. The 2θ scale is calibrated against the Al_2O_3 (012)-peak observed at 25.577°, and the intensity is normalized at the low 2θ side of the peaks. The insets show Gaussian−Lorentzian curves fitted to the two main features in the diffractogram and represent the peaks of (a) an unknown phase and (b) rutile RuO_2.

Included in Figure 2 is the RuO_2 (110) peak from a reference electrode, i.e., a RuO_2/Ni electrode that has not been exposed to electrolyte. The rutile RuO_2 (110) peak of the reference electrode is located at 27.96°. However, while exposed to hydrogen evolution the electrode coating absorbs hydrogen, which is incorporated into the rutile RuO_2 crystal structure.[23] The incorporation of hydrogen, which causes a lattice expansion, is not totally reversible when the cathodic polarization is removed.[23] Hence, after 0.5 h exposure to hydrogen evolution, the rutile RuO_2 (110) peak is shifted to 27.90°, i.e., because of the residual hydrogen in the electrode material there is a 2θ shift of 0.06° for the rutile RuO_2 (110) peak. As the duration of the hydrogen evolution proceeds the rutile RuO_2 (110) peak shows an increasing shift to lower 2θ, accompanied by a decrease in intensity. Simultaneously, a peak from an unknown crystal phase appears, which increases in intensity with the duration of hydrogen evolution. The insets in Figure 2 show Gaussian−Lorentzian (GL) curves obtained from curve fitting of the rutile RuO_2 (110) peak and the unknown phase in the XRD diffractograms. The peak position, full width at half-maximum, and normalized integrated area of the presented GL curves are summarized in Tables 1 and 2 for

Table 1. Parameters Obtained for the Gaussian-Lorentzian Curve Fitting of the RuO_2 (110) Peak

duration [h]	2θ-value [deg]	fwhm[a] [deg]	normalized integrated area
0	27.96 ± 0.01	0.63 ± 0.01	1
0.5	27.90 ± 0.01	0.62 ± 0.01	0.83 ± 0.01
3	27.83 ± 0.01	0.76 ± 0.01	0.58 ± 0.01
6	27.68 ± 0.01	0.90 ± 0.02	0.41 ± 0.01
12	27.45 ± 0.04	1.09 ± 0.07	0.25 ± 0.01
18	27.45 ± 0.07	1.21 ± 0.14	0.21 ± 0.02
24	27.22 ± 0.15	1.32 ± 0.31	0.18 ± 0.03

[a]Full width at half-maximum.

Table 2. Parameters Obtained for the Gaussian-Lorentzian Curve Fitting of the Peak of the Unknown Phase

duration [h]	2θ-value [deg]	fwhm[a] [deg]	normalized integrated area
0			
0.5	27.10 ± 0.01	1.41 ± 0.26	0.25 ± 0.01
3	26.91 ± 0.01	1.34 ± 0.04	0.71 ± 0.07
6	26.69 ± 0.01	1.18 ± 0.04	0.96 ± 0.10
12	26.50 ± 0.01	1.00 ± 0.05	0.99 ± 0.09
18	26.55 ± 0.04	0.97 ± 0.06	0.97 ± 0.07
24	26.48 ± 0.03	0.93 ± 0.05	1

[a]Full width at half-maximum.

the peaks of RuO_2 and the unknown phase, respectively. The GL curves for the RuO_2 (110) peak verify a continuous decrease of the integrated intensity and a shift to lower 2θ. The GL curves for the peak of the unknown phase show initially an increase of the integrated intensity and simultaneously a shift to lower 2θ. However, at extended exposures to hydrogen evolution, i.e., after 6 h, the integrated intensity suggests no further significant growth of the unknown phase.

The integrated intensity for the GL curves of the peaks of the RuO_2 (110) and the unknown phase are shown in Figure 3.

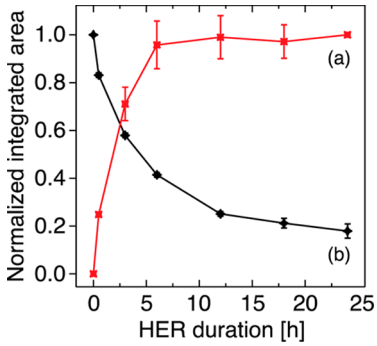

Figure 3. Normalized integrated intensity of the Gaussian−Lorentzian curves that represent the peaks of (a) the unknown phase and (b) the rutile RuO_2.

The most prominent observation is that while the peak of the unknown phase shows no significant increase in size after 6 h of hydrogen evolution, the decrease of the RuO_2 (110) peak continues exponentially. Assuming that the continued consumption of the crystalline RuO_2 after 6 h of hydrogen evolution remains to be because of formation of the unknown crystalline phase, which is reasonable since the exponentially decrease of the RuO_2 (110) peak is not affected when the increase of the peak for the unknown phase levels out, then the lack of increase of the amount of the unknown phase suggest that this too is consumed by a second process forming a second unknown phase, and after 6 h of hydrogen evolution these two processes will reach a stage when the rate of formation and the rate of the consumption of the unknown phase are equal. A wide θ-2θ scan does not indicate any formation of a second unknown phase, which implies that the second unknown phase does not form a crystal phase or that the amount is not large enough to be detected by the present XRD settings. Hence, while the consumption of crystalline RuO_2 occurs through the whole coating, the formation of the second unknown phase suggests being limited to the near surface region of the electrode coating.

dx.doi.org/10.1021/jp503960q | J. Phys. Chem. C 2014, 118, 15315−15323

3.2. X-ray Photoelectron Spectroscopy. From the XRD study we can conclude that the electrode coating, exposed to hydrogen evolution in alkaline media, is subjected to a transformation from the rutile RuO_2 phase into two unknown phases that previously have not been identified. To identify the new phases, we have employed the chemical specific and local geometry sensitive XPS technique.

Figure 4 shows the Ru 3d XPS spectra for the RuO_2/Ni electrodes that have been exposed to hydrogen evolution for

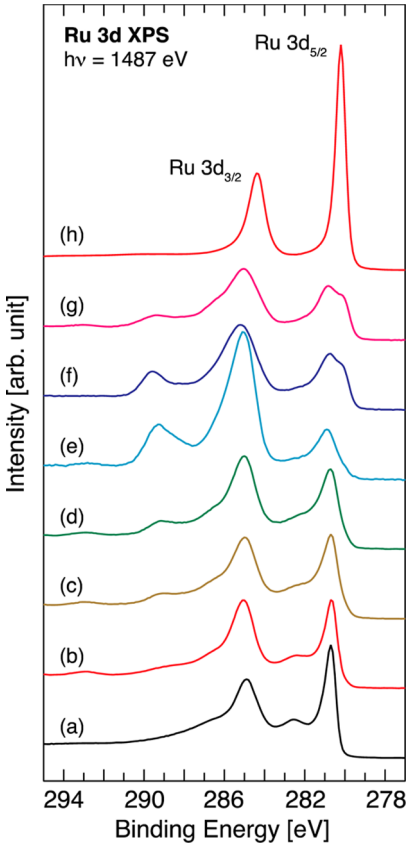

Figure 4. Ru 3d XPS of RuO_2/Ni electrodes exposed to hydrogen evolution for (b) 0.5 h, (c) 3 h, (d) 6 h, (e) 12 h, (f) 18, and (g) 24 h. Included are also the spectra of (a) the reference RuO_2/Ni coating and (h) the Ru-metal.

0.5, 3, 6, 12, 18, and 24 h together with the spectra of the reference RuO_2/Ni coating and the Ru-metal. As clearly illustrated in the figure, exposing the RuO_2/Ni electrode to hydrogen evolution promotes changes in the material, manifested as an intensity redistribution in the Ru 3d XPS spectrum. The redistribution of intensity toward higher binding energies culminates at a hydrogen evolution duration of 12 h, and thereafter the intensity shifts back toward the lower binding energy region. More specific, the trends that are observed, as the hydrogen evolution proceeds, are that the Ru $3d_{5/2}$ peak becomes broader, the Ru $3d_{5/2}$ satellite peak decreases in intensity, the intensity around the Ru $3d_{3/2}$ peak increases at first but decreases after 12 h, the Ru $3d_{3/2}$ peak becomes broader, a growth of a peak at 289.2 eV that reduces in intensity after 12 h, and a growth of a peak at 280.2 eV.

To identify the origin of the intensity redistribution observed in Figure 4, peak fitting is performed for the Ru 3d XPS spectrum of the RuO_2/Ni electrode that has been exposed to hydrogen evolution for 3 h. The spectrum is peak fitted with the use of the experimentally obtained Ru 3d spectra of the reference RuO_2/Ni electrode and the Ru-metal shown in Figure 1, the RuO_2 main peaks obtained from the peak fitting of the reference RuO_2/Ni electrode (see Figure 1), a spectrum of C 1s contamination on TiO_2, and a Shirley background for the peak fitted RuO_2 main peaks. The motivation of including the experimentally recorded spectra of the RuO_2/Ni coating, the Ru-metal, and C 1s contamination on TiO_2 in the peak fitting is based on the fact that the coating still consists of unaltered RuO_2, the position of the growing peak at 280.2 eV line up with the position of the Ru $3d_{5/2}$ for Ru-metal, and C 1s contamination can be expected on samples that have been exposed to atmosphere.[19] The obtained main peaks from the peak fitting of the reference RuO_2/Ni electrode, shown in Figure 1, are included in the peak fitting of the RuO_2/Ni electrode that has been exposed to hydrogen evolution. RuO_2 that has lost charge shows a significant reduction of the satellite feature, and the obtained satellite peaks from the peak fitting of the reference RuO_2/Ni electrode, shown in Figure 1, should therefore not be included.[24]

The result of the peak fitting is presented in Figure 5 and shows that the broadening of the Ru $3d_{5/2}$ can be fitted with

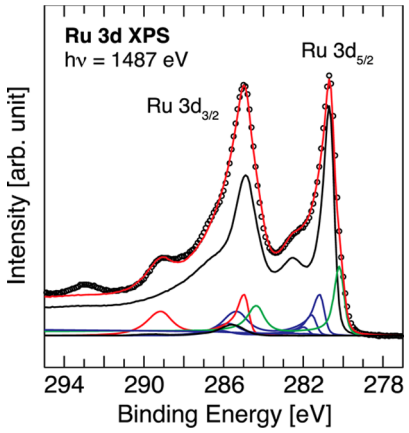

Figure 5. Ru 3d XPS of the RuO_2/Ni electrode exposed to 3 h of hydrogen evolution fitted with spectra of the reference RuO_2/Ni coating (black) and the Ru-metal (green), as shown in Figure 3, the RuO_2 main peaks obtained from the peak fitting of the reference RuO_2/Ni electrode (blue—short BE shift, red—large BE shift), a spectrum of C 1s contamination on TiO_2 (black), and a Shirley background for the peak fitted RuO_2 main peaks (blue).

three spectra of RuO_2 main peaks that are shifted toward higher binding energies by 0.5−1.3 eV, which indicates a charge transfer away from the Ru atom. The charge transfer is most likely a consequence of the incorporated hydrogen that needs to be screened and because of small variations in the position of the hydrogen the interaction with the surrounding Ru atoms will be affected leading to different degree of shift for the Ru $3d_{5/2}$ as well as Ru $3d_{3/2}$. Furthermore, among all the Ru $3d_{3/2}$ components that contribute to the intensity in the region of the Ru $3d_{3/2}$ peak, there is one spectrum of RuO_2 main peaks that is shifted by 4.3 eV, i.e., the RuO_2 $3d_{5/2}$ peak is moved into the RuO_2 $3d_{3/2}$ region. The result from the peak fitting is summarized in Table 3 and suggests that after 3 h of hydrogen evolution 2/3 of the RuO_2 in the probed volume remains unaltered, about 13% of the RuO_2 has lost charge, about 8% of the RuO_2 has transformed into the unknown phase, about 10% of the RuO_2 has been reduced to metallic Ru, and about 2% of

dx.doi.org/10.1021/jp503960q | J. Phys. Chem. C 2014, 118, 15315−15323

Table 3. Result from the Ru 3d Spectrum Peak Fitting of the RuO_2/Ni Electrode that has been Exposed to Hydrogen Evolution for 3 h

component	peak positions[a] [eV] $3d_{5/2}$; $3d_{3/2}$	fraction[b,c]	assigned to
reference RuO_2/Ni coating	280.7; 284.9	0.67	unaltered RuO_2 coating
RuO_2, main peaks 1	281.2; 285.4	0.08	For the RuO_2, main peaks 1−3, the assignment is RuO_2 involved in charge transfer from Ru toward incorporated hydrogen.
RuO_2, main peaks 2	281.6; 285.8	0.04	
RuO_2, main peaks 3	282.0; 286.2	0.01	
RuO_2, main peaks 4	285.0; 289.2	0.08	the unknown phase
Ru-metal	280.2; 284.4	0.10	metallic Ru
C 1s contamination	285.7 (C 1s)	0.02	hydrocarbon (−CH_2− and −CH_3) at 285.7 eV and carboxylate (−COO) at 289.2 eV
	289.2 (C 1s)		

[a]The peak position is determined within ±0.05 eV. [b]The intensity contribution of the added Shirley background is included in the fractions of the four RuO_2 main peaks. [c]The fraction of the reference RuO_2/Ni coating is determined within ±3%. All other fractions are determined within ±20%.

the intensity contribution originates from C 1s contamination (in addition to C 1s contribution that might be hidden in the spectrum of the reference RuO_2/Ni electrode).

A feature that is not included in the peak fitting of the spectrum in Figure 5 is the high binding energy feature around 292.9 eV. This peak is probably a satellite feature of the Ru $3d_{3/2}$ of the unknown phase and a corresponding Ru $3d_{5/2}$ satellite feature would then contribute to intensity around 288 eV where the fitted result now shows a deviation from the XPS spectrum. Except that they most likely have the same origin as the satellite features of RuO_2 and, if so, would contribute to the fraction of the unknown phase, we will not further speculate about the nature of these satellites.

The peak fitting of the Ru 3d spectrum shown in Figure 5 indicates that the unknown phase consists of Ru atoms that, compared to RuO_2, have lost charge and, thus, suggests an increase of oxidation state or hydroxylated (or oxyhydroxylated) Ru species, although the former suggestion can be excluded considering the experimental conditions. The observed shift toward higher binding energy is contra-intuitive since the electrode is operative in a reducing environment. Further chemical information is therefore needed and that can be obtained from the O 1s XPS. It is, however, clear that the unknown phase is an intermediate, and the electrode material will in the end reduce down to metallic Ru as shown by the intensity redistribution toward lower binding energy (see the intensity increase at 280.2 eV in Figure 4).

The O 1s XPS spectra of the RuO_2/Ni electrodes are shown in Figure 6. The O 1s will also go through an intensity redistribution when exposed to hydrogen evolution. The main intensity shifts from 529.5 eV toward higher binding energies and after 24 h of hydrogen evolution the dominating contribution is around 531.5 eV. In the view of the shift toward higher binding energies, it is plausible to suggest that the coating material is hydroxylated (or oxyhydroxylated) and/or hydrated, because O 1s binding energies of Ru−OH and Ru−H_2O is revealed to be 530.8 and 532.8 eV, respectively;[25] after 24 h of hydrogen evolution most of the RuO_2 has been consumed in the near surface region probed by XPS, as shown in Figure 4g, and we can therefore expect a dominant amount of Ru−OH and Ru−H_2O components in the corresponding O 1s spectrum; see Figure 6g.

Peak fitting is performed and presented in Figure 7 for the O 1s XPS spectra of the reference RuO_2/Ni coating and the RuO_2/Ni electrode that has been exposed to hydrogen evolution for 24 h. According to the XRD diffractogram, shown in Figure 2, the selected XPS spectrum of the latter has

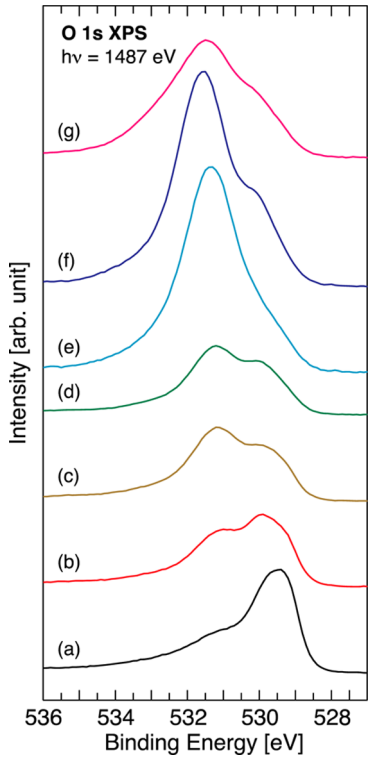

Figure 6. O 1s XPS of RuO_2/Ni electrodes exposed to hydrogen evolution for (b) 0.5 h, (c) 3 h, (d) 6 h, (e) 12 h, (f) 18, and (g) 24 h. Included are also the spectrum (a) the reference RuO_2/Ni electrode.

the highest ratio of the unknown phase compared to RuO_2, which makes the peak fitting easier. However, all oxygen containing species that are present in the near surface region probed by XPS should be included in the peak fitting of the O 1s spectra. We know that the reference electrode coating consists of RuO_2 and NiO and the electrode coating that has been exposed to 24 h of hydrogen evolution consists of RuO_2 and $Ni(OH)_2$; for the determination of the Ni-species; see Figure 8. In addition, adsorbed water can hardly be avoided and should therefore also be included. Finally, based on the obtained results from the Ru 3d spectra, we can expect hydroxylated or oxyhydroxylated Ru-species. Therefore, based on this, we must include one asym-GL curve representing RuO_2, two asym-GL curves representing the Ni-components,[22] one asym-GL curve representing H_2O, and two asym-GL curves representing the unknown phase, i.e., hydroxylated or oxyhydroxylated Ru-species. The minimum number of asym-

dx.doi.org/10.1021/jp503960q | J. Phys. Chem. C 2014, 118, 15315−15323

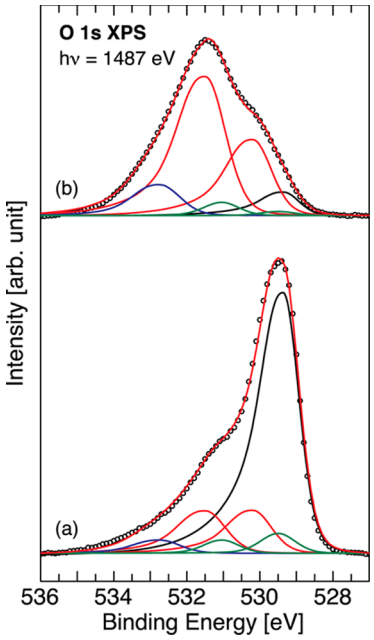

Figure 7. O 1s XPS of (a) the reference RuO_2/Ni coating and (b) the RuO_2/Ni electrode exposed to hydrogen evolution for 24 h. The two spectra are fitted with six asymmetric Gaussian−Lorentzian curves, where one curve represents RuO_2 (black), one curve represent H_2O (blue), two curves represent the Ni−O components[22] (green), and two curves represent the unknown phase (red). Shirley backgrounds are subtracted from the two spectra.

GL curves in the peak fitting of the O 1s spectra must therefore be six. The foremost outcome from the peak fitting is the remarkable decrease of the asym-GL curve that represents RuO_2. Instead the dominating asym-GL curves are the two that represent the unknown phase, where the asym-GL curve assigned to a Ru−O component and the asym-GL curve assigned to a Ru−OH component corresponds to 27% and 51%, respectively, of all oxygen containing species in the near surface region probed by XPS.

The result from the peak fitting is summarized in Table 4 and the obtained peak fitting suggests that RuO_2 is consumed during hydrogen evolution forming an unknown phase that consists of Ru−O and Ru−OH bonds with the ratio 1:2.

That Ni−O components must be included in the peak fitting of the O 1s spectra is motivated from the Ni $2p_{3/2}$ XPS spectra shown in Figure 8. The figure clearly shows that the coating of the reference RuO_2 electrode contains NiO, with the main peaks at 854.2 and 855.9 eV, which after 24 h of hydrogen evolution is transformed into $Ni(OH)_2$ with the main peak at

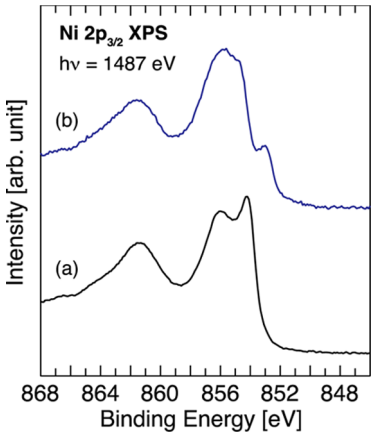

Figure 8. Ni $2p_{3/2}$ XPS of (a) the reference RuO_2/Ni coating and (b) the RuO_2/Ni electrode exposed to hydrogen evolution for 24 h. The two Ni 2p spectra indicate that NiO, which is present in the RuO_2 coating, transforms into $Ni(OH)_2$ and metallic Ni during hydrogen evolution.

855.6 eV;[22,26] the shoulder around 854.7 eV suggest that some NiO still remains. Included in the spectrum of the latter is also a metallic Ni peak at 853.0 eV,[26] which implies reduction of the Ni(II)-component during hydrogen evolution and, thus, supporting the decrease of the Ni−O components in the O 1s spectra of Figure 7.

3.3. Identification of the Unknown Phase. In addition to crystal expansion caused by hydrogen incorporation into the RuO_2 rutile crystal structure,[23] the combined XRD and XPS study shows that RuO_2 coating, when exposed to hydrogen evolution in alkaline medium, is subjected to a transformation into a previously not identified phase, which in turn transforms into metallic Ru. The XRD peak position of the unknown phase is around 26.5°, which coincide with the (101)-peak position of ruthenium oxychloride, $RuOCl_2$,[27] however, RuO_2 coatings prepared from ruthenium nitrosyl nitrate, $Ru(NO)(NO_3)_3$, confirmed that the unknown phase is not $RuOCl_2$.

Peak fitting of the Ru 3d XPS spectrum from a RuO_2/Ni electrode that has been exposed to hydrogen evolution for 3 h shows that the Ru atoms in the unknown phase have lost charge, in comparison to RuO_2, which possibly could be through a hydroxylation process. Furthermore, the peak fitting of the O 1s spectrum of a RuO_2/Ni electrode that has been exposed to hydrogen evolution for 24 h supports the suggestion of a hydroxylation process and that the hydroxylated or oxyhydroxylated Ru-species has twice as many Ru−OH components as the number of Ru−O components. The

Table 4. Result from the O 1s Spectra Peak Fitting of the Reference RuO_2/Ni Coating and the RuO_2/Ni Electrode that has been Exposed to Hydrogen Evolution for 24 h

component[a]	peak position[b] [eV]	fraction,[c] reference[d]	fraction,[c] 24 h HE[e]	assigned to
RuO_2	529.4	0.66	0.07	unaltered RuO_2 coating
unknown phase, curve 1	530.2	0.12	0.27	Ru−O component
unknown phase, curve 2	531.5	0.12	0.51	Ru−OH component
H_2O	532.8	0.03	0.11	adsorbed H_2O[f]
Ni−O, curve 1	529.5	0.04	0.01	Ni−O component[g]
Ni−O, curve 2	531.1	0.03	0.03	Ni−OH component[g]

[a]Components represented by asymmetric Gaussian−Lorentzian curves. [b]The peak position is determined within ±0.05 eV. [c]The fractions of the dominant components are determined within ±3%. All other fractions are determined within ±20%. [d]The reference RuO_2/Ni coating. [e]The RuO_2/Ni electrode that has been exposed to hydrogen evolution for 24 h. [f]Confirmed through ref 25. [g]Confirmed through ref 22.

dx.doi.org/10.1021/jp503960q | J. Phys. Chem. C 2014, 118, 15315−15323

combined XRD and XPS study, thus, demonstrate that the unknown phase is ruthenium oxyhydroxide, $RuO(OH)_2$. The study further shows that $RuO(OH)_2$ decomposes as the hydrogen evolution proceeds and the final compound is metallic Ru, as expected from thermodynamics and anticipated in, e.g., Pourbaix diagrams.[28,29]

The chemical transformation from RuO_2 into $RuO(OH)_2$ seems to occur in a hydrogen-rich environment with a considerably low barrier and activated by the charge transfer from the RuO_2 toward incorporated hydrogen. It is therefore highly plausible that in practical applications, such as an electrocatalytic cathode for hydrogen production in the chlor-alkali process and alkaline water electrolysis, the electrode coating after a run in period consists of mainly $RuO(OH)_2$ through the whole electrode coating. There are, however, no indications for that $RuO(OH)_2$ is less electrocatalytic active compare to RuO_2. Yet, the transformation into $RuO(OH)_2$ can affect other important properties of the electrode coating, e.g., the long-term stability. A recent study shows, for example, that the transformed electrode coating is very sensitive to reverse currents.[30] Further studies are therefore motivated especially when the electrochemical conditions are industrially relevant, i.e., at highly concentrated electrolyte, high temperature, and high current density.

4. CONCLUSIONS

Material characterization of RuO_2/Ni electrodes that have been exposed to hydrogen evolution was performed using X-ray diffraction and X-ray photoelectron spectroscopy. The results support the suggestion that hydrogen incorporation into the RuO_2 coating expands the RuO_2 rutile crystal structure,[23] which is confirmed through a small downshift of the rutile RuO_2 (110) peak. The hydrogen incorporation process induces charge transfer from the RuO_2 toward the incorporated hydrogen. In addition, the positively charged RuO_2 coating transforms into $RuO(OH)_2$, which was revealed through the intensity redistribution from known RuO_2 features in the XRD diffractogram and the Ru 3d and O 1s XPS spectra into features related to the oxyhydoxylated phase.

Hence, the detailed material characterization study provides evidence for RuO_2 consumption on DSA-type electrodes while exposed to hydrogen evolution in industrially relevant conditions, such as alkaline media and a high current density. The phase transformation is in the form of a nonelectrochemical hydroxylation, forming $RuO(OH)_2$. As the hydrogen evolution proceeds the formed $RuO(OH)_2$ reduces to metallic Ru.

AUTHOR INFORMATION

Corresponding Author

*E-mail: lars-ake.naslund@liu.se. Phone: +46 (0)13-28 5733.

Notes

The authors declare no competing financial interest.

ACKNOWLEDGMENTS

The study has partly been accomplished through funding from the European Research Council under the European Communities Seventh Framework Program (FP7/2007-2013)/ERC Grant Agreement No. [258509], the Swedish Research Council (VR) Grant No. 642-2013-8020, and the KAW Fellowship program. S.H. acknowledges funding from the Swedish Research Council (VR) Grant No. 2007-5059.

REFERENCES

(1) Trasatti, S. In *The Electrochemistry of Novel Materials*; Lipkowski, J.; Ross, P. N., Eds.; VCH Publishers: New York, 1994; p 207.
(2) Trasatti, S. Electrocatalysis: Understanding the Success of DSA. *Electrochim. Acta* **2000**, *45*, 2377−2385.
(3) O'Brien, T. F.; Bommaraju, T. V.; Hine, F. *Handbook of Chlor-Alkali Technology. Vol. 1: Fundamentals.*; Springer Science+Business Media: New York, 2005.
(4) O'Brien, T. F.; Bommaraju, T. V.; Hine, F. *Handbook of Chlor-Alkali Technology. Vol. II: Brine Treatment and Cell-Operation.*; Springer Science+Business Media: New York, 2005.
(5) Holladay, J. D.; Hu, J.; King, D. L.; Wang, Y. An Overview of Hydrogen Production Technologies. *Catal. Today* **2009**, *139*, 244−260.
(6) Børresen, B.; Hagen, G.; Tunold, R. Hydrogen Evolution on $Ru_xTi_{1-x}O_2$ in 0.5 M H_2SO_4. *Electrochim. Acta* **2002**, *47*, 1819−1827.
(7) Jovic, V. D.; Lacnjevac, U.; Jovic, B. M.; Kristajic, N. V. Service Life Test of Non-Noble Metal Composite Cathodes for Hydrogen Evolution in Sodium Hydroxide Solution. *Electrochim. Acta* **2012**, *63*, 124−130.
(8) Iwakura, C.; Tanaka, M.; Nakamatsu, S.; Inoue, H.; Matsuoka, M.; Furukawa, N. Electrochemical Properties of Ni/(Ni + RuO_2) Active Cathodes for Hydrogen Evolution in Chlor-Alkali Electrolysis. *Electrochim. Acta* **1995**, *40*, 977−982.
(9) Janjua, M. B. I.; Le Roy, R. L. Electrocatalyst Performance in Industrial Water Electrolysers. *Int. J. Hydrogen Energy* **1985**, *10*, 11−19.
(10) Kötz, E. R.; Stucki, S. Ruthenium Dioxide as a Hydrogen-Evolving Cathode. *J. Appl. Electrochem.* **1987**, *17*, 1190−1197.
(11) Burke, L. D.; Naser, N. S. Metastability and Electrocatalytic Activity of Ruthenium Dioxide Cathodes Used in Water Electrolysis Cells. *J. Appl. Electrochem.* **2005**, *35*, 931−938.
(12) Hachiya, T.; Sasaki, T.; Tsuchida, K.; Houda, H. Ruthenium Oxide Cathodes for Chlor-Alkali Electrolysis. *ECS Trans.* **2009**, *16*, 31−39.
(13) Blouin, M.; Guay, D. Activation of Ruthenium Oxide, Iridium Oxide, and Mixed Ru_xIr_{1-x} Oxide Electrodes during Cathodic Polarization and Hydrogen Evolution. *J. Electrochem. Soc.* **1997**, *144*, 573−581.
(14) Rochefort, D.; Dabo, P.; Guay, D.; Sherwood, P. M. A. XPS Investigations of Thermally Prepared RuO_2 Electrodes in Reductive Conditions. *Electrochim. Acta* **2003**, *48*, 4245−4252.
(15) Mårtensson, N.; Nyholm, R. Electron Spectroscopic Determinations of M and N Core-Hole Lifetimes for the Elements Nb—Te (Z=41−52). *Phys. Rev. B* **1981**, *24*, 7121.
(16) Kim, Y. J.; Gao, Y.; Chambers, S. A. Core-Level X-ray Photoelectron Spectra and X-ray Photoelectron Diffraction of RuO_2(110) Grown by Molecular Beam Epitaxy on TiO_2(110). *Appl. Surf. Sci.* **1997**, *120*, 250−260.
(17) Cox, P. A.; Goodenough, J. B.; Tavener, P. J.; Telles, D. The Electronic Structure of $Bi_{2-x}Gd_xRu_2O_7$ and RuO_2: A Study by Electron Spectroscopy. *J. Solid State Chem.* **1986**, *62*, 360−370.
(18) Hüfner, S. *Photoelectron Spectroscopy: Principles and Applications*, 3rd ed.; Springer-Verlag: Berlin, Heidelberg, 2010; pp 71−76.
(19) Cousens, D. R.; Wood, B. J.; Wang, J. Q.; Atrens, A. Implications of Specimen Preparation and of Surface Contamination for the Measurement of the Grain Boundary Carbon Concentration of Steels Using X-ray Microanalysis in an UHVFESTEM. *Surf. Interface Anal.* **2000**, *29*, 23−32.
(20) Jayaweera, P. M.; Quah, E. L.; Idriss, H. Photoreaction of Ethanol on TiO_2(110) Single-Crystal Surface. *J. Phys. Chem. C* **2007**, *111*, 1764−1769.
(21) Hüfner, S. *Photoelectron Spectroscopy: Principles and Applications*, 3rd ed.; Springer-Verlag: Berlin, Heidelberg, 2010; pp 141−145.
(22) Payne, B. P.; Biesinger, M. C.; McIntyre, N. S. Use of Oxygen/Nickel Ratios in the XPS Characterisation of Oxide Phases on Nickel Metal and Nickel Alloy Surfaces. *J. Electron Spectrosc. Relat. Phenom.* **2012**, *185*, 159−166.

(23) Chabanier, C.; Guay, D. Activation and Hydrogen Absorption in Thermally Prepared RuO_2 and IrO_2. *J. Electroanal. Chem.* **2004**, *570*, 13−27.
(24) Näslund, L.-Å.; Sánchez-Sánchez, C. M.; Ingason, Á. S.; Bäckström, J.; Herrero, E.; Rosen, J.; Holmin, S. The Role of TiO_2 Doping on RuO_2-Coated Electrodes for the Water Oxidation Reaction. *J. Phys. Chem. C* **2013**, *117*, 6126−6135.
(25) Andersson, K.; Nikitin, A.; Pettersson, L. G. M.; Nilsson, A.; Ogasawara, H. Water Dissociation on Ru(001): An Activated Process. *Phys. Rev. Lett.* **2004**, *93*, 196101.
(26) Grosvenor, A. P.; Biesinger, M. C.; Smart, R.; St, C.; McIntyre, N. S. New Interpretations of XPS Spectra of Nickel Metal and Oxides. *Surf. Sci.* **2006**, *600*, 1771−1779.
(27) Hillebrecht, H.; Schmidt, P. J.; Rotter, H. W.; Thiele, G.; Zoennchen, P.; Bengel, H.; Cantow, H.-J.; Magonov, S. N.; Whangbo, M.-H. Structural and Scanning Microscopy Studies of Layered Compounds MCl_3 (M = Mo, Ru, Cr) and $MOCl_2$ (M = V, Nb, Mo, Ru, Os). *J. Alloys Compd.* **1997**, *246*, 70−79.
(28) Pourbaix, M. *Atlas of Electrochemical Equilibria in Aqueous Solutions*, Engl. Ed.; Pergamon Press: Oxford, 1966.
(29) Takeno, N. *Atlas of Eh-pH Diagrams; Intercomparison of Thermodynamic Databases*, Geological Survey of Japan Open File Report No. 419; National Institute of Advanced Industrial Science and Technology, Research Center for Deep Geological Environments: Tsukuba, Japan, 2005.
(30) Holmin, S.; Näslund, L.-Å.; Ingason, Á. S.; Rosen, J.; Zimmerman, E. Corrosion of Ruthenium Dioxide Based Cathodes in Alkaline Medium Caused by Reverse Currents, 2014, submitted for publication.